Supplementary Figures

Supplementary Fig. 1. Frequency distribution for sites below the detection limit for different production cohorts of non-low production sites
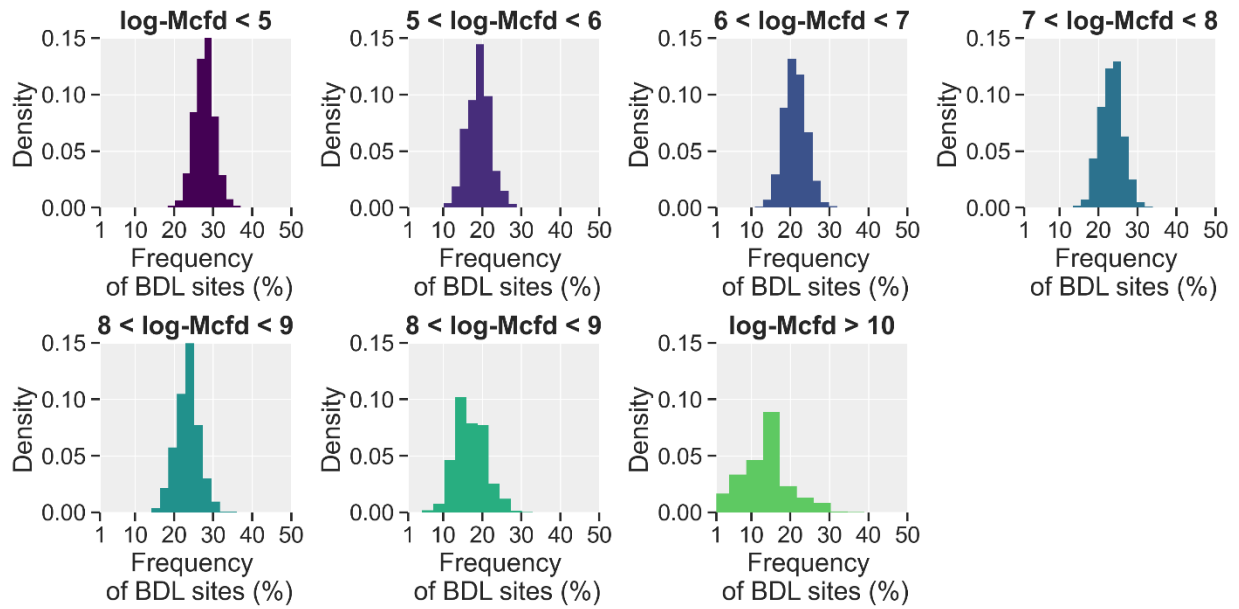
10

15

Supplementary Fig. 2: Random samples drawn from the modeled distribution for each production cohort, showing good agreement between modeled and empirical distributions.
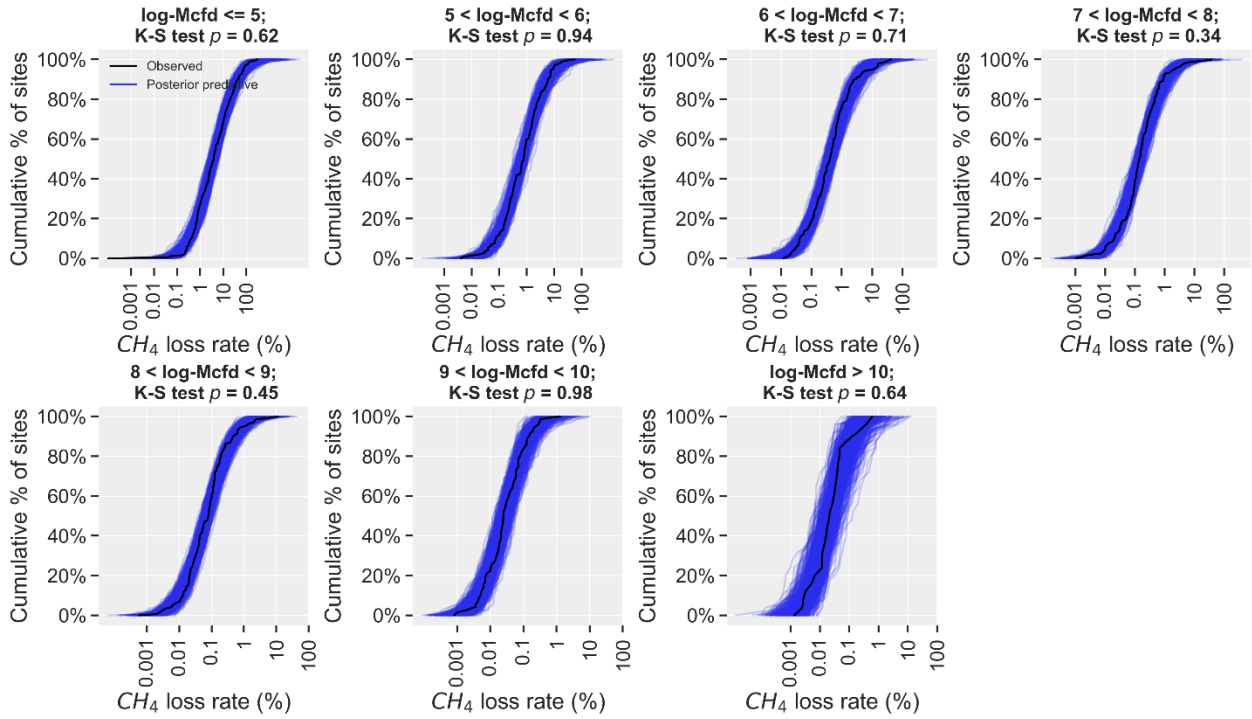
Supplementary Fig. 3: Comparison of facility-level gas production rates for the measured non-low production sites and the national population of well sites.
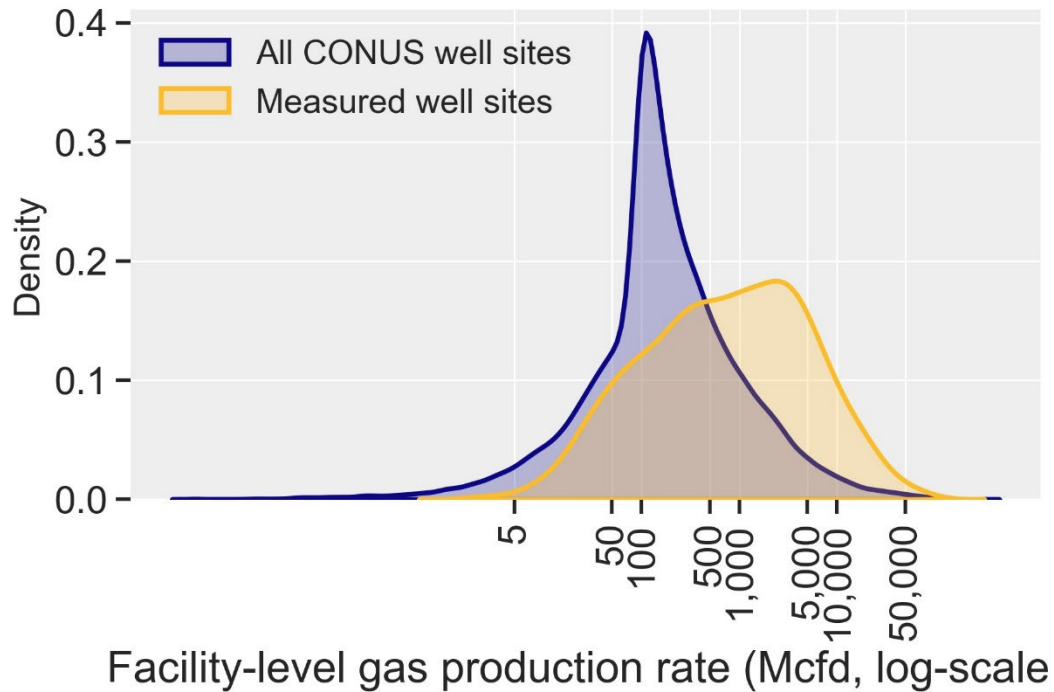
Supplementary Fig. 4. Top 6 emitting basins in EI-ME. Map credit: ESRI, 2023.
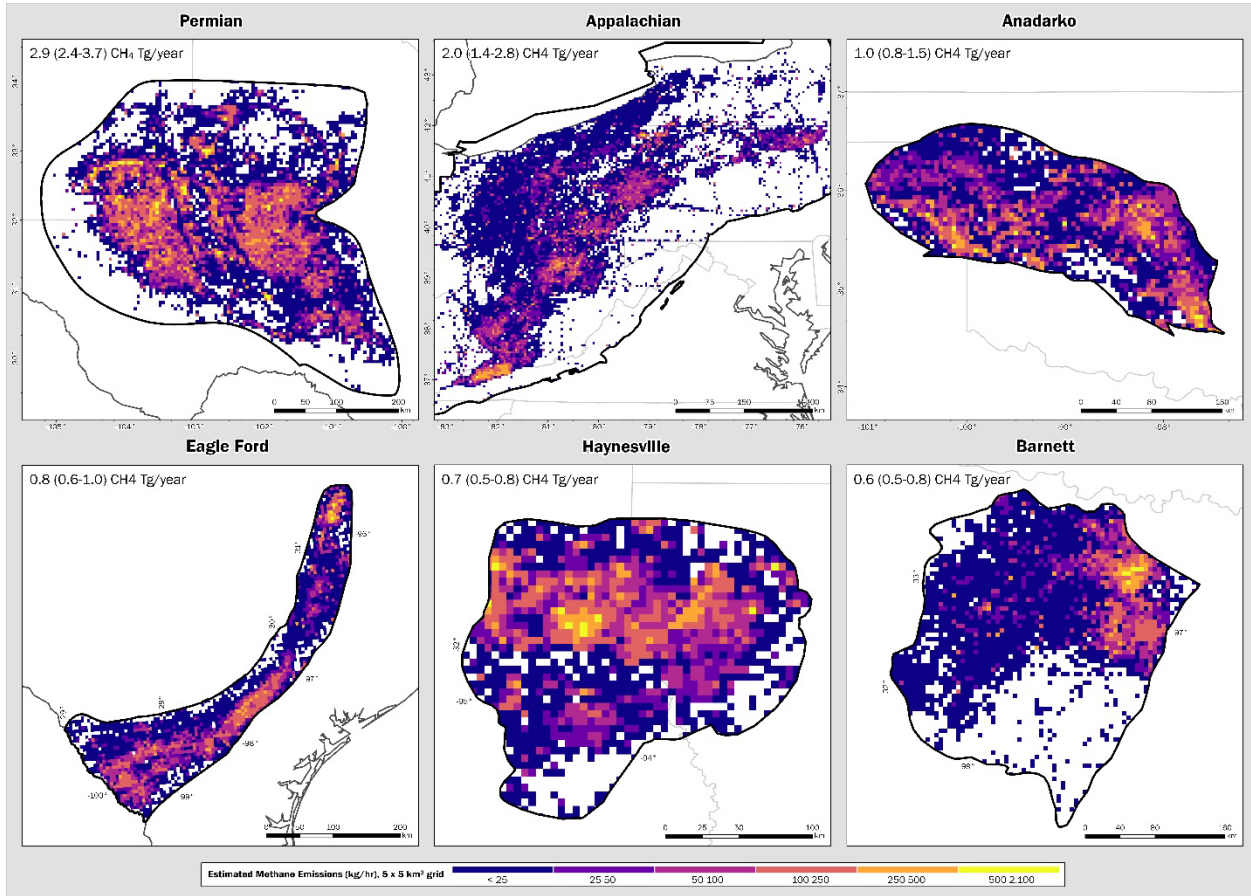
Supplementary Fig. 5. Comparison of oil and gas activity data for the top five CONUS oil and gas production basins in 2021. Map credit: ESRI, 2023.
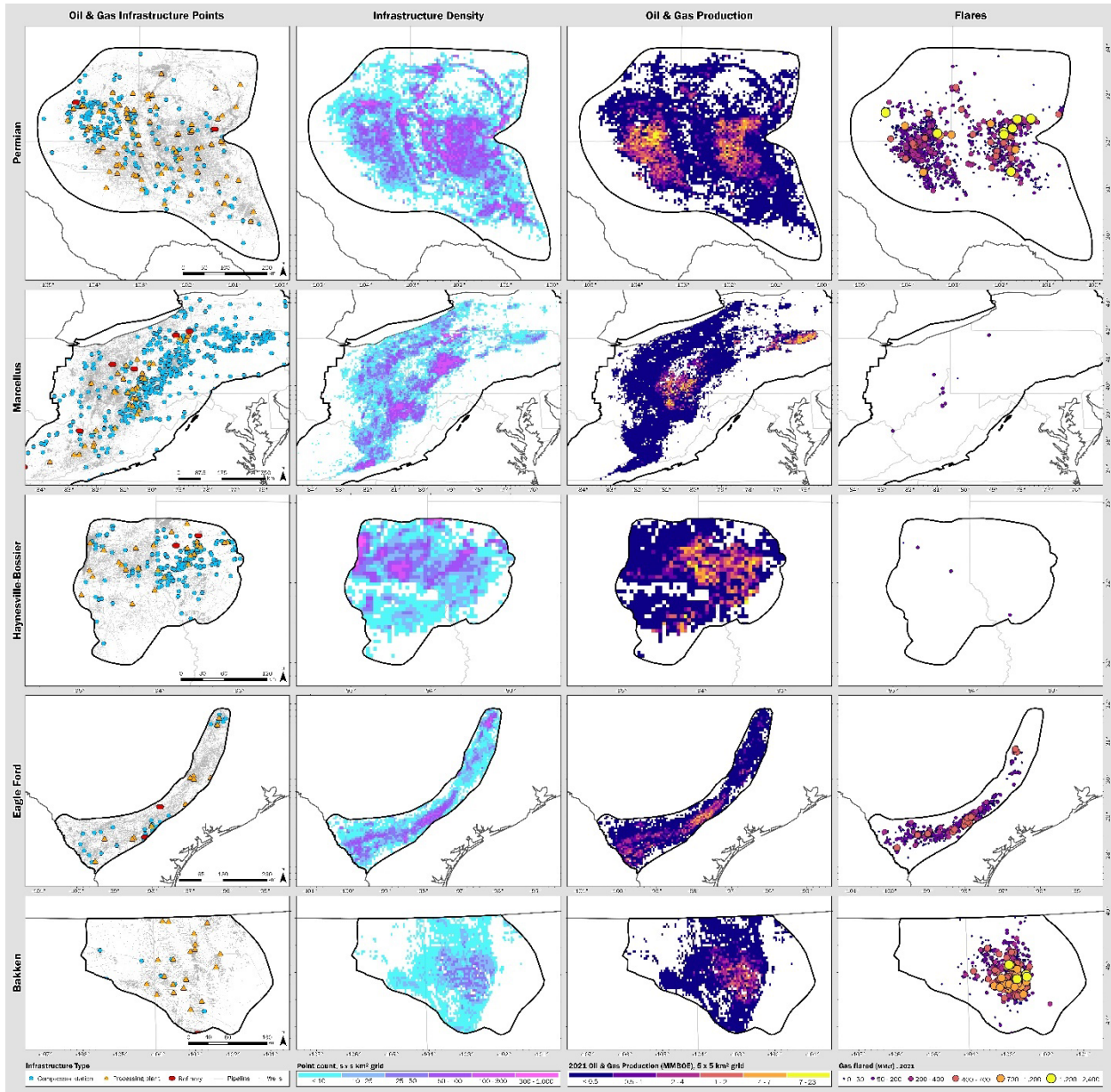
Supplementary Fig. 6. Spatial distribution comparison of top 3 emitting basins in EI-ME and EPA GHGI estimates. Map credit: ESRI, 2023.
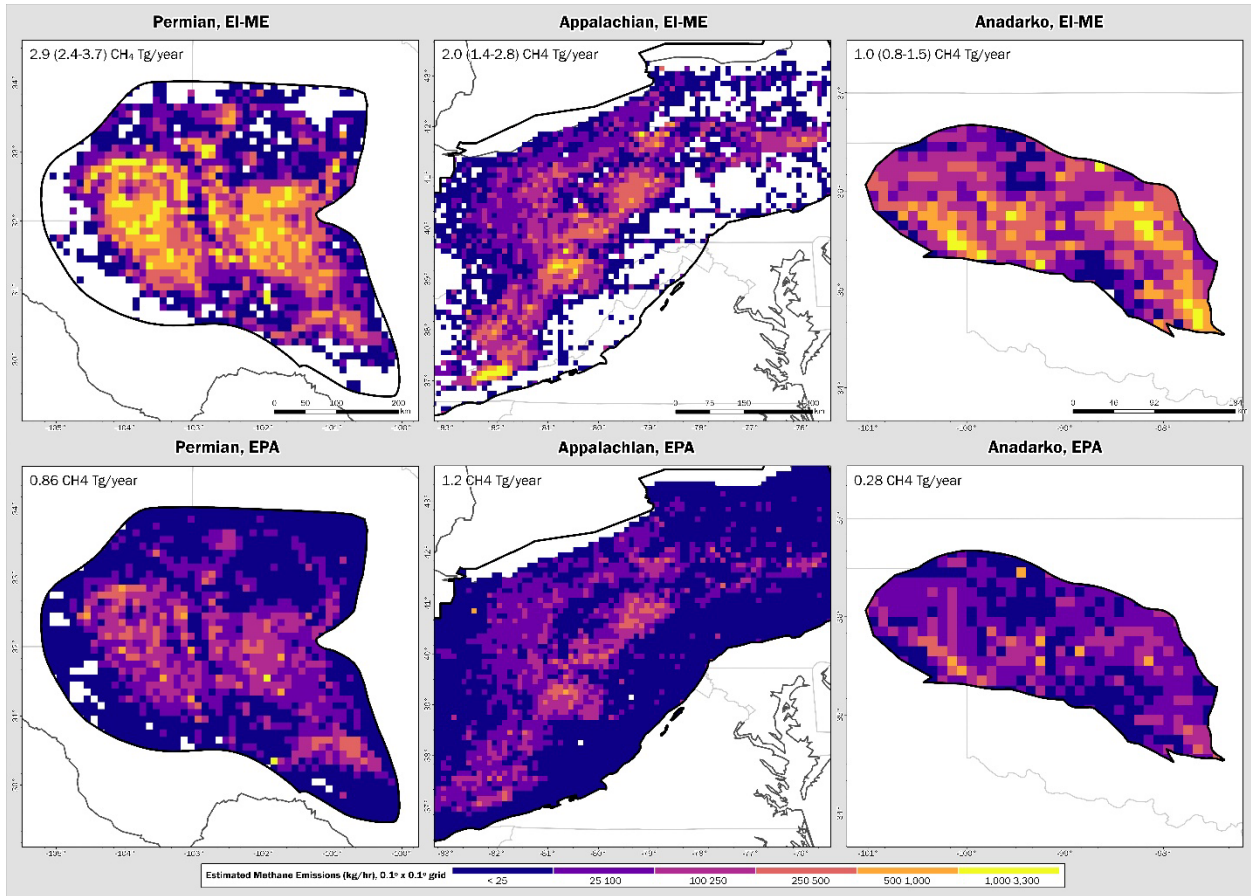
Supplementary Fig. 7. Difference in estimated spatial distribution of methane emissions between this study and the EDGAR v8 inventory.
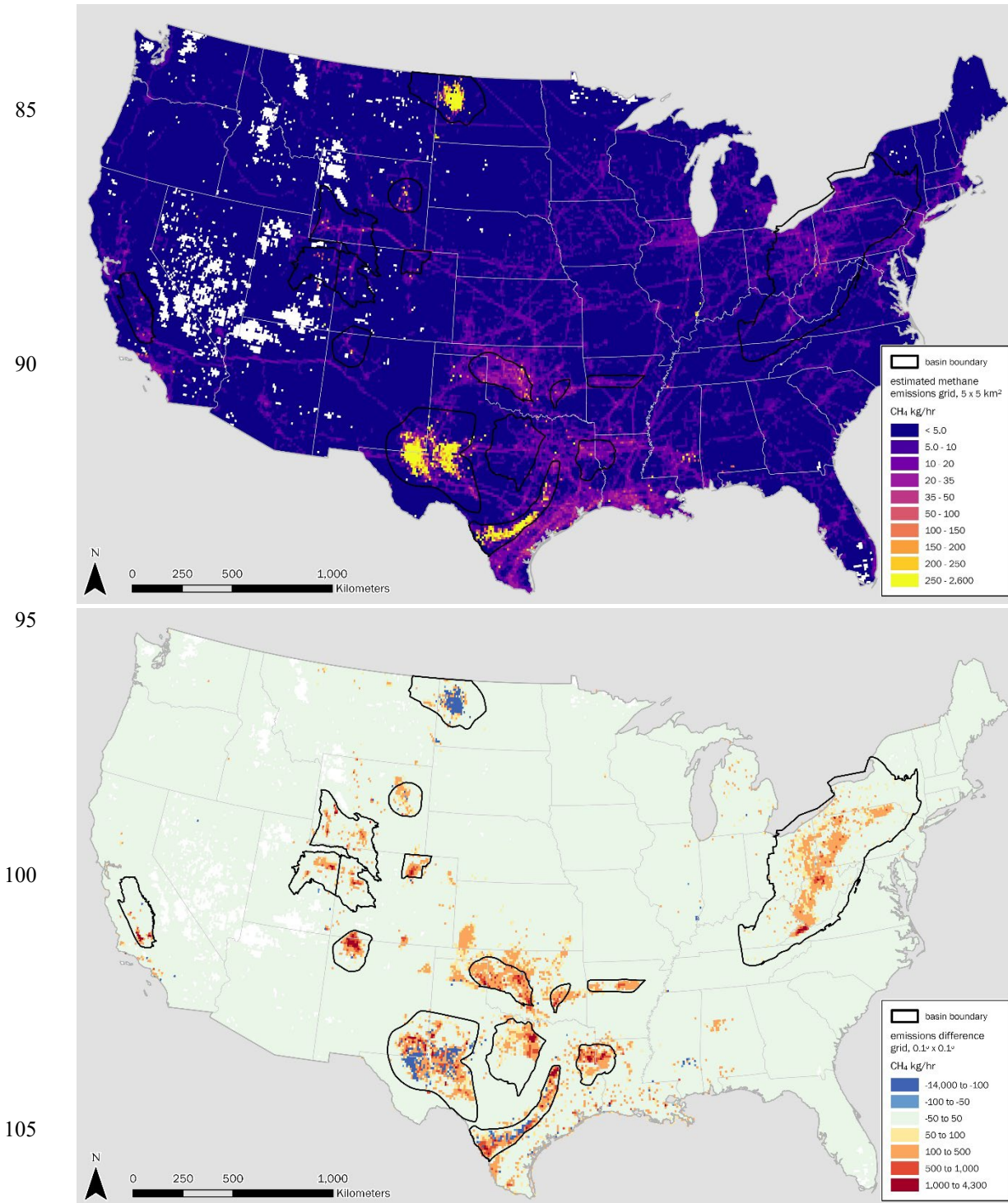
a. Estimated spatial distribution of methane emissions in the EDGAR v8 inventory, showing large methane hotspots in the oil-dominant basins of the Permian, Eagle Ford, and the Bakken. **b.** Difference in spatially explicit methane

110 emissions between this study's measurement-based inventory and the EDGAR v8 inventory, showing large differences in all of the major oil and gas basins. Map credit: ESRI, 2023.